

Seismic Pattern and Co-seismic Stress of Aftershock Sequences in the mainland Southeast Asia

Premwadee Traitangwong* and Santi Pailoplee

Morphology of Earth Surface and Advanced Geohazards in Southeast Asia Research Unit (MESA RU), Department of Geology, Faculty of Science, Chulalongkorn University, Bangkok 10330, Thailand

* Corresponding author e-mail: traitangwong.p@gmail.com

Abstract

This study focuses on analyzing the characteristics of the aftershock in the MSEA due to the magnitude of the aftershock that occurred after the 2004 Sumatra mainshock, equivalent to the magnitude of the 2011 Tarlay mainshock. The seismicity of aftershock sequences for the 13 seismic source zones proposed in the MSEA was analyzed by estimated the fractal dimension (D_c) and the frequency–magnitude distribution (a and b values) and which is used only the aftershock data. After estimated, the obtained D_c value can be implied the behavior of the distribution of aftershock sequences in the MSEA, whereas the obtained b value can be implied the co-seismic stress for aftershock sequences. In addition, the empirical relationships of D_c and b values and D_c value with a/b ratios for the aftershock sequence are different from the relationships for mainshock, where both the relationships are positive correlation, with $D_c = 0.13b + 2.07$ and $D_c = 0.21(a/b) + 0.98$, respectively. In case of the regression coefficients of both correlations, for the aftershock are less than for the mainshock. Therefore, the both relationships of mainshock were more reliable and effective than the both relationships of aftershock in the MSEA.

Key words: Aftershock Sequence, Fractal Dimension, Frequency-Magnitude Distribution, Mainland Southeast Asia

1. Introduction

The mainland Southeast Asia (MSEA) is considered as one of the most seismically active in any region of the world (Pailoplee and Choowong, 2014) because of the catastrophe caused by the M_w -9.0 earthquake generated on December 26th, 2004 at off the coast of Sumatra in western Indonesia. Moreover, after this earthquake occurs, then it caused the M_w -6.9 aftershock in same area, which compared with the M_w -6.9 mainshock earthquake at Tarlay city, Myanmar.

Up to the present, there are several statistical seismology techniques to analyze the characteristic of seismicity. In this study, fractal dimension (D_c value) (Grassberger and Procaccia, 1983) and frequency–magnitude distribution (a and b values) (Gutenberg and Richter, 1944) were used in the assessment. The D_c value is obtained using the correlation

integral mode that analyze the spatial distribution of seismicity and directly controlled by the heterogeneity of the stress zone and the precedent geological structures (Oncel et al., 1996). The b value is related to the distribution of stress (Scholz, 1968). From the previous research, it found that the relationships of the D_c - b values and the D_c -(a/b) ratios in several regions of the worlds (Hirata, 1989; Barton et al., 1999; Bhattacharya et al., 2010; Bayrak and Bayrak, 2012; Yadav et al., 2012). In addition, Pailoplee and Choowong (2014) was calibrated both relationships for the mainshock in the MSEA.

It can be seen that not only does the mainshock caused damage and fatalities, but the aftershock also affected as same as. Therefore, we are interested in evaluating parameters, i.e. a , b and D_c values, as well as the relationships of the D_c - b values and the D_c value with a/b ratios for the aftershock sequence in all seismic source

zones proposed in the MSEA. The obtained results will help to fulfill the both relationships of D_c - b values and D_c value- (a/b) ratios for aftershock in the MSEA, which can imply seismic hazard.

2. Seismic Source and Seismicity

2.1 Seismic source

Tectonically, the MSEA region is located on the Eurasian and Indo-Australian plates (Polachan et al., 1991; Fenton et al., 2003) that Indo-Australian plate move to beneath Eurasian

plate has caused several major earthquakes in the region. Based on the previous research, the seismic source zones in the MSEA have been proposed in several studies in order to analyze the seismic hazards in this area. For example, Nutalaya et al. (1985) proposed 12 seismic source zones, then Charusiri et al. (2005) revised and proposed 21 seismic source zones. After that, Pailoplee and Choowong (2013) is re-grouped and re-located the seismic source zone that proposed 13 new zones in the MSEA.

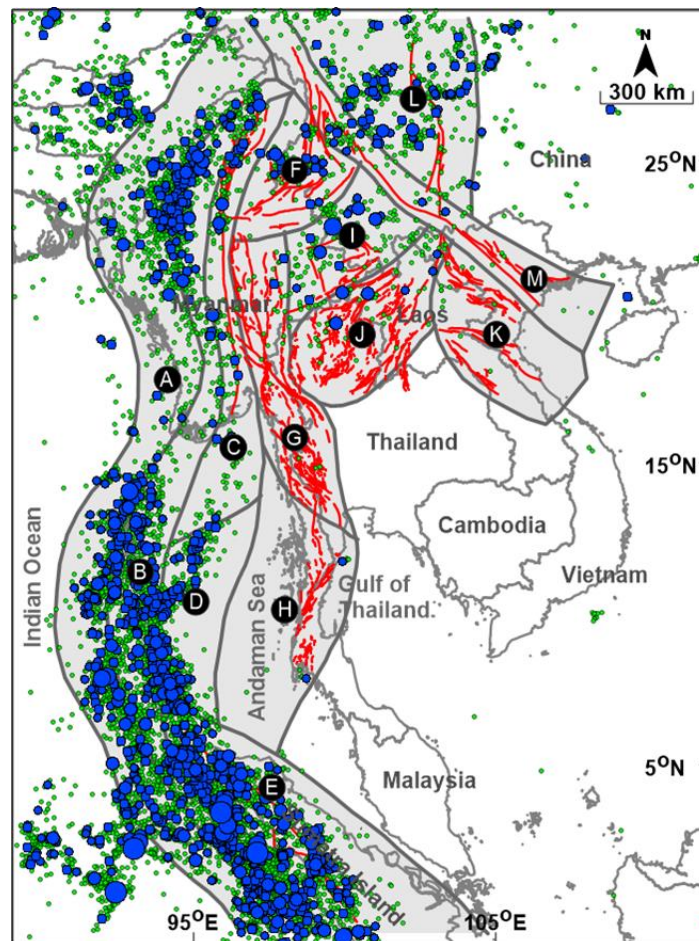


Figure 1. Map of the mainland Southeast Asia (MSEA) and the 13 seismic source zones composed of zone A to M showing the distributions of the mainshocks during the 1985–2017, which is represented by varies size of blue circles according to magnitude and all of aftershocks (green circles). Red lines indicate the fault lines compiled by Pailoplee et al. (2009) and grey

polygons depict the geometry of the individual zones proposed by Pailoplee and Choowong (2013).

Table 1. Parameters of Gutenberg-Richter relationship (a and b values) and fractal dimensions (D_c) of the 13 seismic source zones (zone A–M) in the mainland Southeast Asia (MSEA).

Name	a	b	M_c	D_c
(A) Sumatra-Andaman Interplate	6.84	1.12 ± 0.2	4.5	2.23 ± 0.01
(B) Sumatra-Andaman intraslab	6.85	1.02 ± 0.1	4.5	2.57 ± 0.01
(C) Sagaing Fault Zone	7.18	1.22 ± 0.3	4.9	1.96 ± 0.02
(D) Andaman Basin	6.62	1.16 ± 0.2	4.4	2.26 ± 0.01
(E) Sumatra Fault Zone	7.23	1.17 ± 0.1	4.5	2.20 ± 0.01
(F) Hsenwi-Nanting Fault Zone	6.24	1.03 ± 0.4	4.1	N/A
(G) Western Thailand	N/A	N/A	N/A	N/A
(H) Southern Thailand	N/A	N/A	N/A	N/A
(I) Jinghong-Mengxing fault zones	6.81	1.11 ± 0.4	4.9	2.05 ± 0.01
(J) Northern Thailand-Dein Bein Phu	5.92	1.12 ± 0.4	4.3	N/A
(K) Song Da-Song Ma fault zones	N/A	N/A	N/A	N/A
(L) Xianshuihe Fault Zone	5.39	0.91 ± 0.2	4.3	2.12 ± 0.02
(M) Red River Fault Zone	N/A	N/A	N/A	N/A

After that, Pailoplee and Choowong (2013) is regrouped and re-located the seismic source zone that proposed 13 new zones in the MSEA. In this study chose to divided into 13 seismic source zone (zone A-M) according to Pailoplee and Choowong (2013) (Figure 1; Table 1) which the detail can be explained as follow.

The Sumatra-Andaman subduction zone is related to the interaction between the Eurasian plate and Indo-Australian collision zone that separate to 2 seismotectonic setting as follows. The Sumatra-Andaman interplate (zone A) is generated a shallow-focus earthquakes while the Sumatra-Andaman intraslab (zone B) is

generated an intermediate to deep-focus earthquakes (>35 km.) under the western Myanmar, Sumatra and Nicobar Islands (Paul et al., 2001).

In addition to the Sumatra-Andaman subduction zone, the Sagaing fault zone (zone C) is a dextral strike-slip active fault zone that trending north-south direction in the central part of Myanmar. The slip rate of this fault is 23 mm/yr (Bertrand and Rangin, 2003).

Zone D, the Andaman basin is interpreted as the backarc region in the Sumatra-Andaman subduction zone which has the active east-west

rifting process until now (Rajendran et al., 2003; Khana and Chakraborty, 2005).

Whereas, the major strike-slip faults that located on the southern portion of Sumatra-Andaman intraslab is called the Sumatra fault zone (zone E). This fault zone has direction in northwest-southeast in Sumatra island.

There are two systems of strike-slip fault along the Thailand-Laos-Myanmar borders. First, the northwest-southeast strike-slip faults are defined as zone G that consist of i) Sri Sawat fault (Nuttee et al., 2005), ii) Moei-Tongyi fault (Pailoplee et al., 2009) and iii) Three Pagoda fault (Rhodes et al., 2005). And second, the northeast-southeast strike-slip faults are located between southern of Thailand and Myanmar that including the Ranong and Klong Marui fault zones are grouped into zone H.

In the northern Thailand, there are some active faults such as the Phrae (Udchachon et al., 2005), Lampang-Theon (Charusiri et al., 2004) and Mae Tha fault zones (Rhodes et al., 2004) that are defined as zone J or the northern Thailand-Dein Bein Phu (Pailoplee and Choowong, 2013).

For the southern China, northern Vietnam, northern Myanmar and northern Laos are located in the northern part of the MSEA which relate to the Eurasian and Indo-Australian plate collision that cause of the northeast-southwest and northwest-southeast complex shear zone and the strike-slip fault (Polachan et al., 1991). The seismic source zones in this region consist of the Hsenwi-Nanting fault zones (zone F) and Jinghong-Mengxing fault zones (zone I) (Lacassin et al., 1998).

In the eastern part of the MSEA, there are many fault zones such as the Song Da, Song Ma fault (Phoung, 1991), Song Ca fault (Takemoto

et al., 2005) and Song Chay fault (Cuong and Zuchiewicz, 2001) which lies in the NW-SE direction along the northern Vietnam. In this region, all fault zones are classified as the earthquake source zones, namely Song Da-Song Ma fault zones (zone K). Furthermore, the eastern part of the MSEA has the significant fault zone which namely the Red River fault zone that lies along the China-Vietnam border with 810 km. (Duong and Feigl, 1999). This fault zone is defined as the seismic source zone namely zone M.

The last seismic source zone in the MSEA region which relate to the Eurasian plate is the Xianshuihe fault zone (zone L) located on the southern China that lies in north-south direction (Eleftheria et al., 2004).

2.2. Seismicity

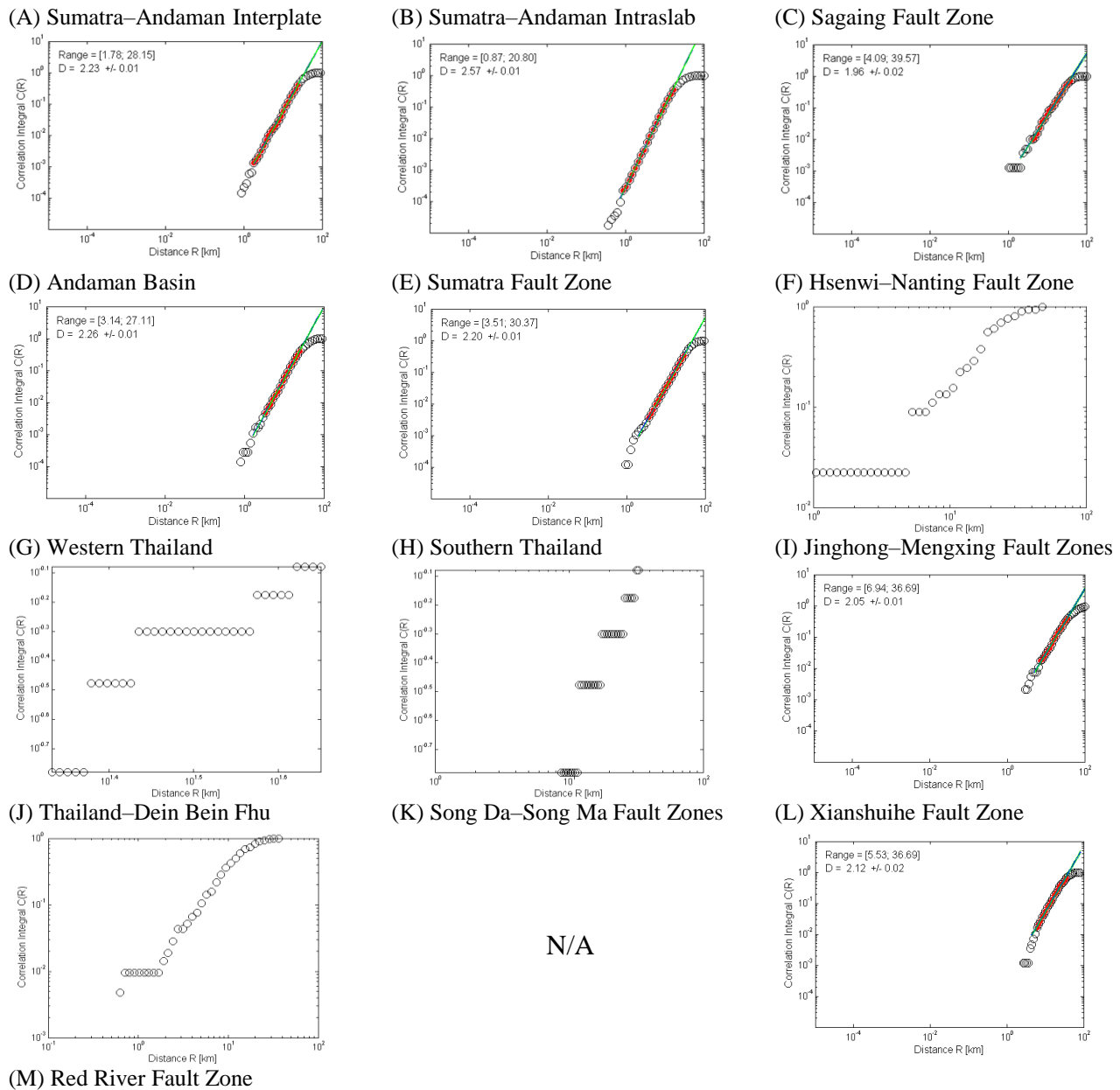
In case of seismicity recognized in this study, the instrumentally recorded earthquakes were taken as the dataset. The earthquake catalogue used in this study were obtained by the US National Earthquake Information Center (NEIC), which covers the latitude between 4°N - 33°N and the longitude between 86°E - 115°E (Figure 1). The earthquake catalogue consists of 20,115 earthquake events recorded during from January 1st, 1985 to August 31st, 2017, which reported in the different magnitude scales. In case of qualitative statistical seismicity analysis, homogeneous seismicity scale is necessary. Thus, the different magnitude scales including body-wave magnitude (m_b) and surface-wave magnitude (M_s) were converted to M_w following the relationship between M_w and m_b , including M_w and M_s , using all the earthquake catalogue in this study as shown in Equations 1-2.

$$M_w = -0.002m_b^2 + 0.640m_b^2 + 2.043 \quad (1)$$

$$M_W = -0.078M_S^2 + 2.132M_S^2 - 4.123 \quad (2)$$

In order to identify the aftershocks within earthquake catalogues, this study uses the window technique, which consider both the space and time windows proposed by Gardner

and Knopoff (1974). As a result, the MSEA consists of 1,697 clusters of 12,489 aftershock (Figure 1). These catalogue is used here to investigate the statistical values of a, b and Dc of the aftershock, as described in the next section.



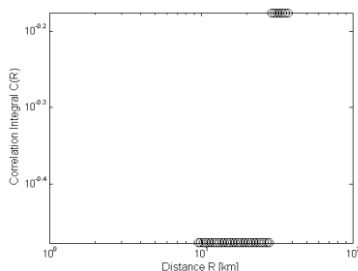


Figure 2. Graphs of the log-log plot of $C(r)$ against r . The fractal dimension (D_c) of the aftershock data for all seismic source zones (zone A–M) in the MSEA is obtained as the slopes of linear fit (solid black lines).

3. Fractal Dimension

The spatial distribution of seismicity is examined by the natural way that called fractal dimension (D_c value). It describes the seismic pattern of the aftershock clusters in the earthquake. This study is used the correlation integral technique to investigate the fractal dimension (Grassberger and Procaccia, 1983), expressed as

$$C(r) = \frac{2}{N(N-1)} N(R < r), \quad (3)$$

where N is the number of earthquakes investigated and $N(R < r)$ is the number of event pairs with a distance R smaller than r . If the epicenter distribution is fractal, the correction will follow the equation 3 (Kagan and Knopoff, 1980).

$$C(r) \sim r^{(D_c)} \quad (4)$$

Where D_c is the correlation fractal dimension that can be evaluated by fitting the data with the slope in line from the log-log plot of $C(r)$ against r . Based on Tosi (1998), the D_c values are in ranges 0 to 2 related with the seismologically active sources. According to Khattri (1995) and Yadav et al. (2011), D_c value will be interpreted differently, as D_c approach zero, the distribution of all events is concentrated in one point. In case of D_c close to 1, the distribution of events will be

approach into line. If close to 2 indicates that the distribution of events is distributed to plane pattern. When close to 3, it can be indicated that the earthquake fractures are filling up a crustal volume.

Based on the previous work, the D_c graphs have been plotted for all seismic source zones in the MSEA (Pailoplee and Choowong, 2014), but the D_c values are derived only from the mainshock data. Thereby, the fractal dimension graphs for the aftershock sequence for the 13 seismic source zones in the MLSEA, which shown in Figure 2 can be estimated the D_c values as shown in Table 1.

After estimating the fractal dimension, D_c value cannot estimate in zone f, g, h, j, k and m due to the lack of available earthquake catalogue (<30 events). All other zones, the calculated D_c values were within the range of 1.96 to 2.57 which is considered that the D_c value approaches 2 in all seismic source zone. The highest D_c value found in zone B ($D_c=2.57$), while the lowest D_c value found in zone C ($D_c=1.96$).

In order to compare the obtained D_c values of aftershock (in this study) and of mainshock (Pailoplee and Choowong, 2014). In this study, we separated the D_c values into four groups, according to Pailoplee and Choowong (2014) that compose of $D_c < 1.5$, $1.5 \leq D_c < 1.7$,

$1.7 \leq D_c < 1.9$ and $D_c \geq 1.9$. As a results shown the various colors mapped in Figure 3. All of D_c values of the aftershock are similar with the highest D_c values ($D_c \geq 1.9$).

According to Yadav et al. (2011), Pailoplee and Choowong (2014) and Ansari (2017), the epicenters of earthquake are homogeneously distributed over a two-dimensional (2-D) fault plane due to a D_c value close to 2. Therefore, it can be implied that the behavior of the aftershock sequences in the

MSEA are distributed into two-dimensional fault plane.

4. Gutenberg-Richter Relationship

The magnitude-frequency relationship is a power law of size distribution during the aftershock that is well described by Gutenberg and Richer (1944)

$$\log(N) = a - bM \quad (5)$$

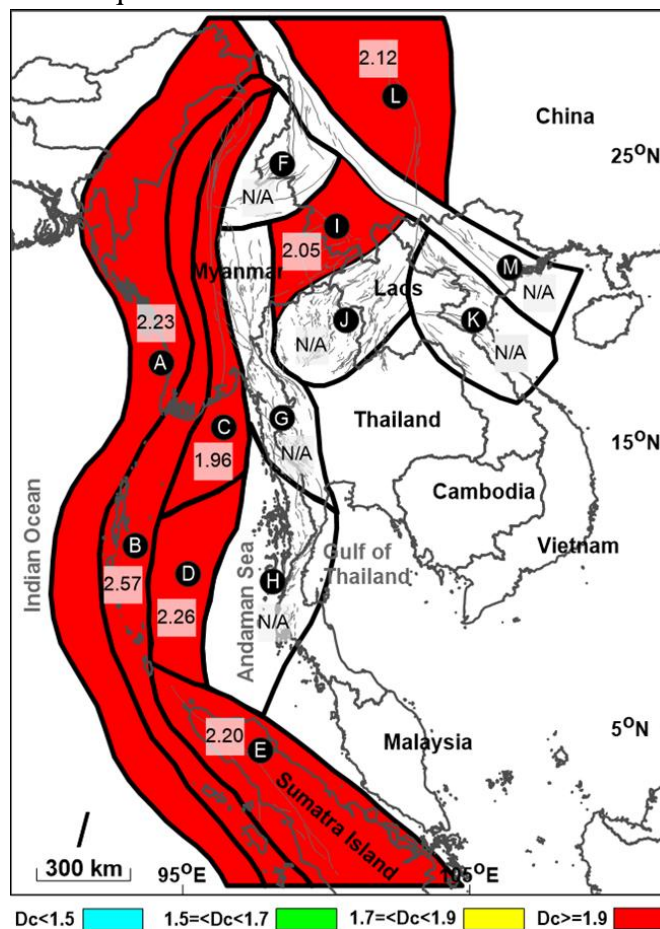


Figure 3. Map illustrating the distributions of the calculated D_c values for the 13 seismic source zones (zone A–M) in the mainland Southeast Asia (MSEA), scaling from Pailoplee and Choowong (2014).

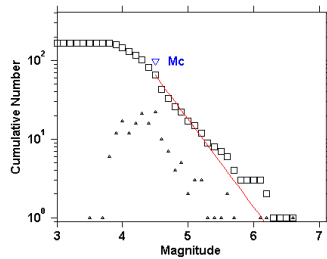
where N is the cumulative number of earthquake with magnitude equal to or greater than M , and a and b are empirical constants vary in a specific time and window. The parameter a describes the seismic activity, whereas the parameter b not only relates the relative occurrence of small to large earthquake but also describes the stress condition. Higher b values related to decrease the accumulated stress (Scholtz, 1968; Wyss, 1973).

From the previous work (Pailoplee and Choowong, 2014), it was found that there was a plot of the G-R relationship for 13 seismic

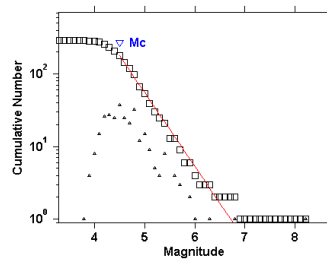
source zones in the MLSEA from the mainshock data as well as the D_c -values. In order to evaluate the G-R relationship of the aftershock sequence, so in this study, only using the aftershock data. As a result, a and b values of G-R relationship of the aftershock was calculated shown in Figure 4 and Table 1.

After the G-R relationship calculation, zone G, H, K and M cannot estimate the G-R relationship plots because the earthquake data is insufficient for analysis.

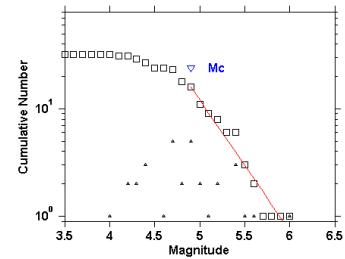
(A) Sumatra–Andaman Interplate



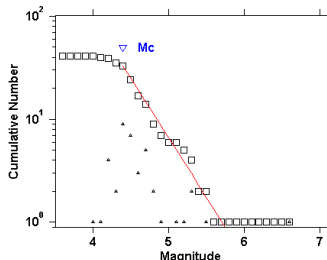
(B) Sumatra–Andaman Intraslab



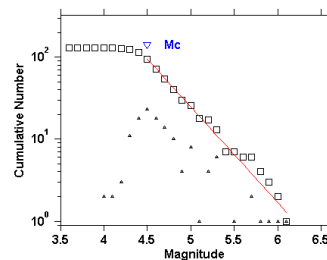
(C) Sagaing Fault Zone



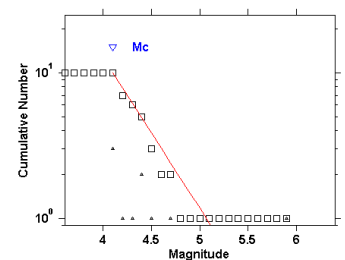
(D) Andaman Basin



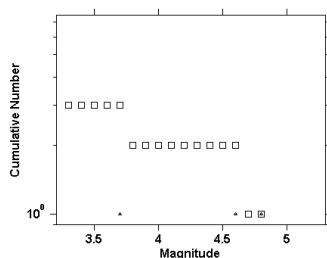
(E) Sumatra Fault Zone



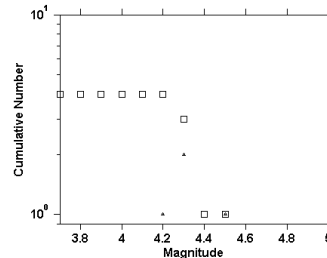
(F) Hsenwi–Nanting Fault Zone



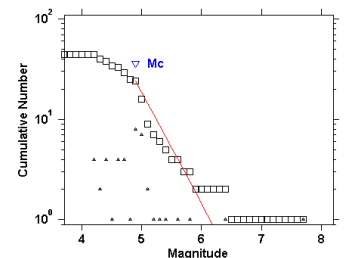
(G) Western Thailand



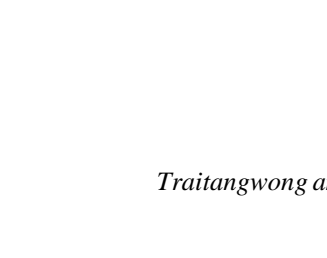
(H) Southern Thailand



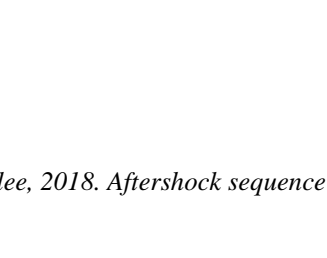
(I) Jinghong–Mengxing Fault Zones



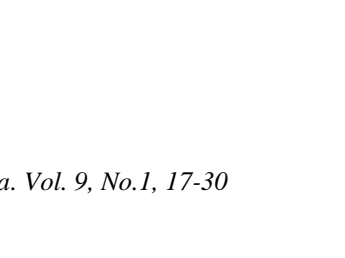
(J) Thailand–Dein Bein Phu

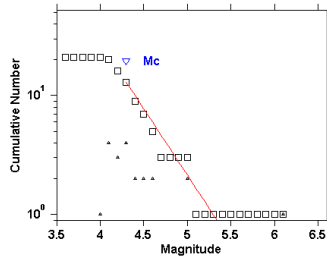


(K) Song Da–Song Ma Fault Zones



(L) Xianshuihe Fault Zone





(M) Red River Fault Zone

N/A

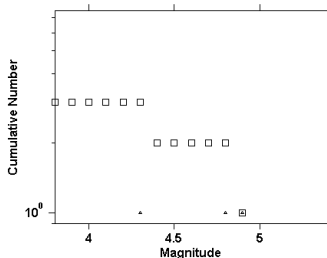
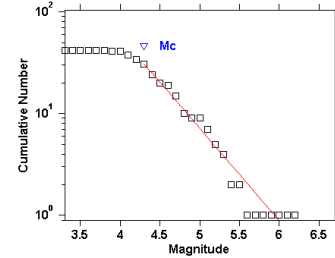


Figure 4. Plots of frequency-magnitude distribution for the 13 seismic source zones (zone A—M). The number and cumulative number of each individual magnitude represent by triangles and squares, respectively. The line represents the maximum likelihood methods used for estimate of a and b value. MC shows the magnitude of completeness (Woessner and Wiemer, 2005).

Overall, in the other zones, calculated b values ranged from 0.91 to 1.22. The highest b value found in zone C ($b=1.22$) while the lowest b value was found in zone L ($b=0.91$).

In order to compare the obtained b values of aftershock (in this study) and of mainshock (Pailoplee and Choowong, 2014). Regarding to the division of the b values into four groups of Pailoplee and Choowong (2014) that consists of $b < 0.7$, $0.7 \leq b < 0.8$, $0.8 \leq b < 0.9$, and $b \geq 0.9$. As a result in this study, the b value of aftershock is shown in different color by these four groups (Figure 5). All of the calculated b values of the aftershock in 13 seismic source zones in the MSEA was observed in the highest group ($b \geq 0.9$) defined by Pailoplee and Choowong (2014) with the a values range in 4.90-8.56 (Table 1). This means that most of the b value calculated from aftershock are higher than b value calculated from mainshock in all zones of the MSEA.

Seismotectonically, the mainshock refers directly to the released tectonic stress (Scholtz, 1968; Wyss, 1973). Whereas, the aftershock is a co-seismic stress change of the mainshock

(Felzer et al., 2004). It can be concluded that co-seismic stress in the MSEA is always lower than the seismotectonic stress because the b value of the aftershock (co-seismic stress) is higher than the b value of the mainshock (seismotectonic stress).

5. D_c -b Relationship

In this study, the relationship between the D_c and b values was determined because this relationship was a significant determinant of seismic hazards (Bayrak and Bayrak 2011, 2012). In practice, the relationship of D_c -b can be either a positive or a negative correlation. For instance, a positive correlation was determined for the earthquake active source zone in the northern and western India (Bhattacharya et al., 2010; Yadav et al., 2012), while a negative correlation was defined for the earthquake source zone in Japan (Hirata, 1989) and Long Valley Caldera in California (volcanic earthquakes) (Barton et al., 1999). From the previous works, Pailoplee and Choowong (2014) were calibrated the correlation between D_c and b values in the MSEA, but this correlation applies to the mainshock. Therefore, this study chose to

calibrate the empirical relationship of D_c - b values that using the aftershock data. Based on the calculated D_c and b values as shown in Table 1, the statistical relationship between D_c and b values can be expressed as

$$D_c = 0.13b + 2.07 \quad (6)$$

The relationship of D_c and b values of the aftershock in the MSEA showed a positive linear regression that shown in Figure 6a.

Moreover, the empirical relationship between D_c values and a/b ratios were calibrated shown in Figure 6b and can be expressed as

$$D_c = 0.21(a/b) + 0.98 \quad (5)$$

Figure 6 illustrates a comparison of the relationship between D_c - b values and D_c value with a/b ratios of the aftershock, which shows the positive correlation for both relationships.

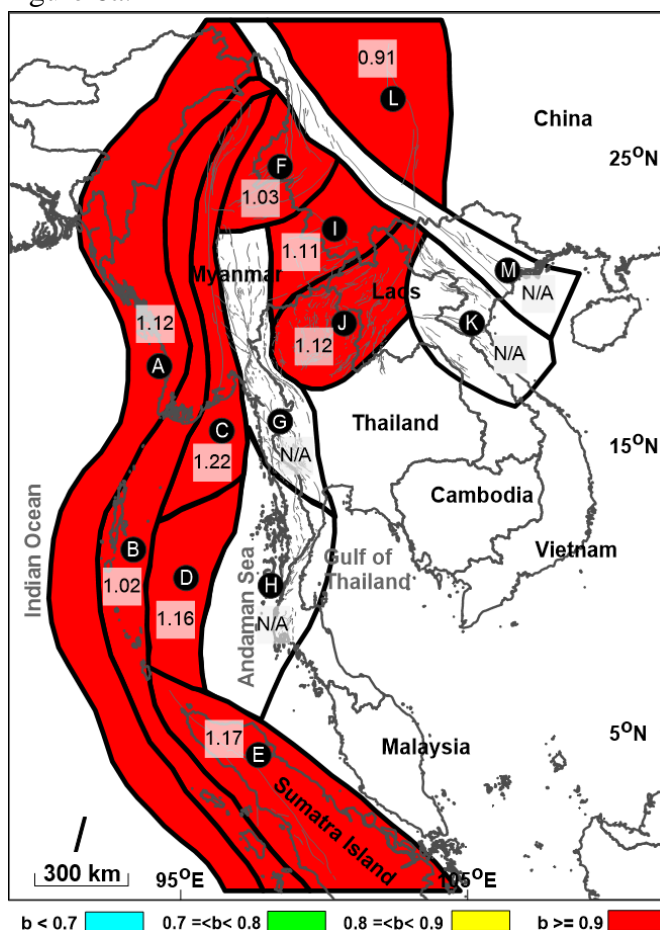


Figure 5. Map illustrating the distributions of the calculated b values for the 13 seismic source zones (zone A–M) proposed in the mainland Southeast Asia (MSEA), scaling from Pailoplee and Choowong (2014).

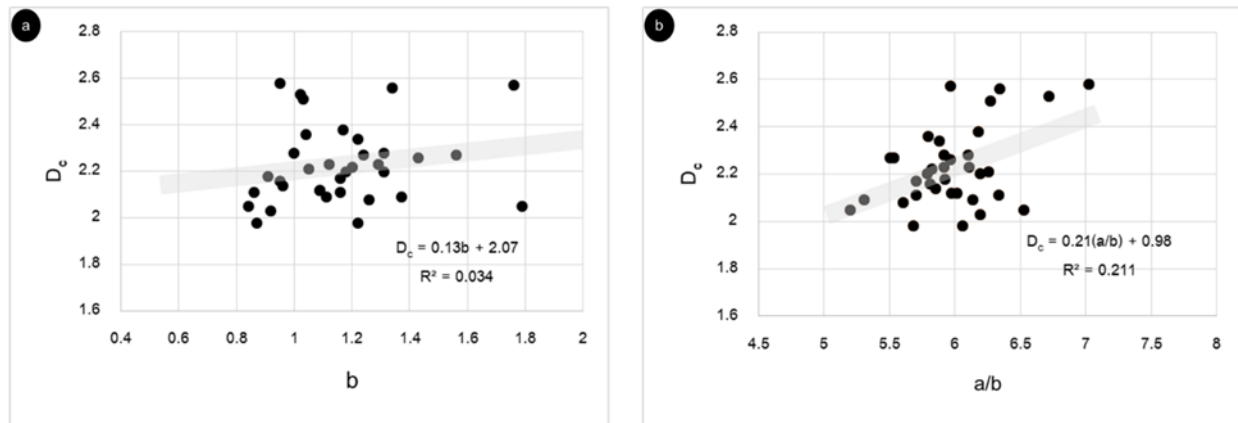


Figure 6. Plot of the empirical correlations between (a) the D_c and b values and (b) the D_c values and a/b ratios for the 13 seismic source zones (zone A–M). The straight lines represent the linear regressions fitted with the aftershock data.

Unlike Pailoplee and Choowong (2014), the D_c - b relationship is a negative correlation, whereas the relationship of D_c value with a/b ratios is a negative correlation. For correlation coefficient, the correlations of mainshock (0.65–0.68) are greater than of the correlations of aftershock (0.03–0.21). Therefore, the both relationships of mainshock were more reliable and effective than the both relationships of aftershock in the MSEA.

6. Conclusion and Remarks

In this study, the fractal dimension and the G-R relationship were analyzed for 13 seismic source zones in the MSEA by using only aftershock data recorded within the study area. The results show the spatial variations of the D_c and b values for aftershock, which can indicate the seismic pattern and co-seismic stress. From the estimated D_c values of the aftershocks, in the MSEA, almost the aftershocks are homogeneously distributed into two-dimensional fault plane. Based on a comparison of the b value between in this study and Pailoplee and Choowong (2014), the b value calculated from aftershock are higher than b value calculated from mainshock in all zones of the MSEA.

Moreover, it is also that the co-seismic stress in the MSEA is always lower than the tectonic stress, which means that the stress released when the mainshock occurs.

According to the correlations of D_c and b values and D_c value with a/b ratios in the MSEA, for the aftershock shows that both of the relationships were positive correlation. Unlike the relationships for mainshock from Pailoplee and Choowong (2014), which found that the D_c and b values relationship was negative regression. In case of the correlation coefficient (R^2 values), this study found that R^2 values are less than. Thereby, the both relationships of mainshock can be used as a more significant determinant of seismic hazards than the both relationships of aftershock in the MSEA.

7. Acknowledgments

This research was funded by the Ratchadapisek Sompoch Endowment Fund (2017), Chulalongkorn University (760003-CC). We also acknowledge the thoughtful comments and suggestions by the BEST journal editor and anonymous reviewers, which significantly enhanced the quality of this manuscript.

8. References

- Barton, D.J., Foulger, G.R., Henderson, J.R., and Julian, B.R. 1999. Frequency-magnitude statistics and spatial correlation dimensions of earthquakes at Long Valley Caldera, California, *Geophys. J. Int.*, 138, 563–570.
- Bayrak, Y. and Bayrak, E. 2011. An evaluation of earthquake hazard potential for different regions in Western Anatolia using the historical and instrumental earthquake data, *Pure. Appl. Geophys.*, 169, 1859–1873.
- Bayrak, Y. and Bayrak, E. 2012. Regional variations and correlations of Gutenberg–Richter parameters and fractal dimension for the different seismogenic zones in Western Anatolia, *J. Asian Earth. Sci.*, 58, 98–107.
- Bertrand, G. and Rangin, C. 2003. Tectonics of the western margin of the Shan Plateau (central Myanmar): implications for the India-Indochina oblique convergence since the Oligocene, *J. Asian Earth. Sci.*, 21, 1139–1157.
- Bhattacharya, P.M., Kayal, J.R., Baruah, S., and Arefiev, S.S. 2010. Earthquake Source zones in Northeast India: Seismic Tomography, Fractal Dimension and b Value Mapping, *Pure Appl Geophys.*, 167, 8, 999–1012.
- Charusiri, P., Choowong, M., Charoentitirat, T., Jankaew, K., Chutakositkanon, V., and Kanjanapayont, P. 2005. Geological and physical effect evaluation in the tsunami damage area for restoration and warning system, Technical report, Department of Geology, Faculty of Science, Chulalongkorn University, Bangkok, Thailand, 412p (in Thai with English abstract).
- Charusiri, P., Daorerk, V., Choowong, M., Muangnoicharoen, N., Won-in, K., Lumjuan, A., Kosuwan, S., Saithong, P., and Thonnarat, P. 2004. The study on the investigations of active faults in Changwat Kanchanaburi area, western Thailand, Technical report, Department of Geology, Faculty of Science, Chulalongkorn University, Bangkok, Thailand, 119p (in Thai with English abstract).
- Cuong, N.Q. and Zuchiewicz, W.A. 2001. Morphotectonic properties of the Lo River Fault near Tam Dao in North Vietnam, *Nat Hazard Earth Syst Sci.*, 1, 15–22.
- Duong, C.C. and Feigl, K.L. 1999. Geodetic measurement of horizontal strain across the Red River fault near Thac Ba, Vietnam. *J Geod.*, 73, 298–310.
- Eleftheria, P., Xueze, W., Vassilios, K., and Xueshen, J. 2004. Earthquake Triggering along the Xianshuihe fault zone of Western Sichuan, China. *Pure Appl Geophys.*, 161, 8, 1683–1707.
- Felzer, K. R., Abercrombie, R.E., and Ekstrom, G. 2004. A common origin for aftershocks, foreshocks, and multiplets. *Bull. Seismol. Soc. Am.*, 94, 88–98.
- Fenton, C.H., Charusiri, P., and Wood, S. 2003. Recent paleoseismic investigations in Northern and Western Thailand, *Ann Geophys.*, 46, 5, 957–981.
- Gardner, J.K. and Knopoff, L. 1974. Is the sequence of earthquakes in Southern California, with aftershocks removed, Poissonian?, *Bull. Seismol. Soc. Am.*, 64, 1, 363–367.
- Grassberger, P. and Procaccia, I. 1983. Measuring the strangeness of strange attractors, *Physica, D9*, 189–208.

- Gutenberg, B. and Richter, C.F. 1944. Frequency of earthquakes in California, *Bull. Seismol. Soc. Am.*, 34, 185-188.
- Hirata, T. 1989. Fractal dimension of fault system in Japan: Fractal structure in rock fracture geometry at various scales, *Pure Appl. Geophys.*, 131(1/2), 157-170.
- Kagan, Y.Y. and Knopoff, L. 1980. Spatial distribution of earthquakes: the two-point correlation function, *Geophys. J. Roy. Astron. Soc.*, 62, 303-320.
- Khana, P.K. and Chakraborty, P.P. 2005. Two-phase opening of Andaman Sea: a new seismotectonic insight, *Earth Planet Sci Lett.*, 229, 259-271.
- Khatti, K.N. 1995. Fractal description of seismicity of India and inferences regarding earthquake hazard. *Current Science*, 69, 361-366.
- Lacassin, R., Replumaz, A., and Leloup, P.H. 1998. Hairpin river loops and strike-slip sense inversion of Southeast Asian strike-slip faults, *Geology* 26, 703-706.
- Nutalaya, P., Sodsri, S., and Arnold, E.P. 1985. Series on Seismology-Volume II-Thailand. In E.P Arnold (ed.), Technical report, Southeast Asia Association of Seismology and Earthquake Engineering, 402p.
- Nuttee, R., Charusiri, P., Takashima, I., and Kosuwan, S. 2005. Paleo-earthquakes along the southern segment of the Sri Sawat Fault, Kanchanaburi, Western Thailand: Morphotectonic and TL-dating evidences, *Proceedings of the International Conference on Geology, Geotechnology and Mineral Resources of Indochina, Khon Kaen, Thailand*, 542-554.
- Öncel, A.O., Main, I., Alptekin, Ö., and Cowie, P. 1996. Temporal variations in the fractal properties of seismicity in the north Anatolian fault zone between 31OE and 41 OE, *Pure Appl. Geophys.*, 147, 147-159.
- Pailoplee, S. and Choowong, M. 2013. Probabilities of earthquake occurrences in Mainland Southeast Asia, *Arabian J. Geosci.*, 6, 4993-5006.
- Pailoplee, S. and Choowong, M. 2014. Earthquake frequency-magnitude distribution and fractal dimension in mainland Southeast Asia, *Earth Planet Sci Lett.*, 66, 8p.
- Paul, J., Burgmann, R., Gaur, V.K., Bilham, R., Larson, K.M., Ananda, M.B., Jade, S., Mukal, M., Anupama, T.S., Satyal, G., and Kumar, D. 2001. The motion and active deformation of India, *Geophys Res Lett.*, 28, 647-650.
- Phoung, N.H. 1991. Probabilistic assessment of earthquake hazard in Vietnam based on seismotectonic regionalization, *Tectonophysics*, 198, 81-93.
- Polachan, S., Pradidtan, S., Tongtaow, C., Janmaha, S., Intrawijitr, K., and Sangsuwan, C. 1991. Development of Cenozoic basins in Thailand, *Mar. Petrol. Geol.*, 8, 84-97.
- Rhodes BP, Charusiri, P., Kosuwan, S., and Lamjuan, A. 2015. Tertiary evolution of the Three Pagodas Fault, Western Thailand. *Proceedings of the International Conference on Geology, Geotechnology and Mineral Resources of Indochina, Khon Kaen, Thailand*, 498-505.
- Rhodes, B.P., Perez, R., Lamjuan, A., and Kosuwan, S. 2004. Kinematics and tectonic implications of the Mae Kuang Fault,

northern Thailand, *J. Asian Earth. Sci.*, 24, 1, 79–89.

Scholz, C.H. 1968. The frequency–magnitude relation of microfracturing in rock and its relation to earthquakes, *Bull. Seismol. Soc. Am.*, 58, 399–415.

Takemoto K, Halim, N., Otofujii, Y., Tran, V.T., Le, V.D., and Hada, S. 2005. New paleomagnetic constraints on the extrusion of Indochina: Late Cretaceous results from the Song Da terrane, northern Vietnam, *Earth Planet Sci Lett.*, 229, 273–285.

Tosi, P. 1998. Seismogenic structure behavior revealed by spatial clustering of seismicity in the Umbria- Marche Region (central Italy), *Ann. Geophys.*, 41, 215–224.

Udchachon, M., Charusiri, P., Daorerk, V., Wonin, K., Takashima, I. 2015. Paleo-seismic studies along the southeastern portion of the Phrae Basin, Northern Thailand, *Proceedings of the International Conference on Geology, Geotechnology and Mineral Resources of Indochina*, Khon Kaen, Thailand, p.511-519.

Yadav, R.B.S., Papadimitriou, E.E., Karakostas, V.G., Rastogi, B.K., Shanker, D., Chopra, S., Singh, A.P., and Kumar, S. 2011. The 2007 Talala, Saurashtra, western India earthquake sequence. Tectonic implications and seismicity triggering, *J. Asian Earth. Sci.*, 40, 1, 303–314.

Yadav, R.B.S., Gahalaut, V.K., Chopra, S., and Shan, B. 2012. Tectonic implications and seismicity triggering during the 2008 Baluchistan, Pakistan Earthquake Sequence, *J. Asian Earth. Sci.*, 45, 2, 167–178.